Non-Markovian dynamics of a single excitation within many-body dissipative systems

Adam Burgess[1,2,3,*] and Marian Florescu[2,3,†]

[1]*Leverhulme Quantum Biology Doctoral Training Centre, University of Surrey, Guildford GU2 7XH, United Kingdom*
[2]*Advanced Technology Institute, University of Surrey, Guildford GU2 7XH, United Kingdom*
[3]*Department of Physics, University of Surrey, Guildford GU2 7XH, United Kingdom*

(Received 26 November 2021; revised 23 March 2022; accepted 12 May 2022; published 7 June 2022)

We explore the dynamics of N coupled atomic two-level systems embedded within a generic bosonic reservoir under specific system symmetries. In the regime of many atoms identically coupled to a single reservoir, we identify remarkable effects, notably that the initial configuration of the atomic excited-state amplitudes strongly impacts the dynamics of the system and can even fully sever the system from its environment. Additionally, we find that steady-state amplitudes of the excited states become independent of the specific structure of the bosonic reservoirs considered. The framework introduced is deployed to model a structured photonic reservoir associated with a photonic crystal, where it recaptures previous theoretical and experimental results for the superradiance rates even within the single-excitation regime. For the photonic band-gap system, our formalism predicts the generation of pairwise entanglement between initially uncorrelated atomic systems. Furthermore, it suggests that—with respect to a non-Markovian metric—the non-Markovianity of the aggregated many-atom system is modulated by the total number of atoms. This is due to a stark interplay between the Lamb shifting of the atomic transition energies due to their varying number and the increased number of atomic systems with resonant transition energies.

DOI: 10.1103/PhysRevA.105.062207

I. INTRODUCTION

Recently, the interest in deploying quantum technologies to go beyond current computational approaches has experienced rapid growth. This has mainly been driven by advances in the capabilities and design of larger quantum computers [1] as well as the developments in quantum algorithm designs that have the capabilities to undermine modern cryptographic methods [2–5]. However, a major difficulty in utilizing such quantum implementations is their proclivity to decohere and dissipate into the environment. In this context, understanding how the environment impacts the evolution of quantum systems along with developing capabilities to control this impact is of vital importance for the next advances in the quantum technologies field [6]. Furthermore, understanding the dynamics of atomic systems within dissipative environments has played a pivotal role in developing new and better artificial structures that have the capacity for processing information on shorter spatial and temporal scales [7–9]. The conventional approach to studying such systems is to deploy the theory of open quantum systems [10], wherein the archetypal model of spin systems coupled to bosonic reservoirs are utilized to model two-level atomic systems coupled to quantized electromagnetic fields. Unravelling the combined dynamics of the two systems is exceedingly difficult and often it is merely the dynamics of the atomic system that is of interest. Therefore, a scheme is required to reduce out the environmental degrees of freedom. A common approach to achieving this is by invoking the Markov approximation, which is valid for environments that recover instantaneously from interacting with the system [11]. Although this approach has proven fruitful in understanding many systems it fails to adequately capture quantum induced memory effects in the system. For example, within microstructured photonic systems, such as photonic crystals, the local density of states for the electromagnetic field varies rapidly for frequencies near the band edges of the photonic band gap. Such rapid fluctuations make the Markov approximation invalid [12–14], and embedding a two-level atomic system with its transition energy near the band edge of a photonic band-gap results in highly non-Markovian dynamics. The strong interaction between the atomic system and the photonic reservoir leads to a dressing of the atomic states highly intertwining the attributes of the photonic reservoir and the atomic degrees of freedom and thus leading to temporal oscillations and fractional decay of atomic population, spectral splitting, and subnatural linewidths of the atomic transitions [15].

Moreover, as we begin to scale up the technology of these artificial systems, it becomes necessary to understand the collective effects of many atomic systems coupled to electromagnetic reservoirs. Recently, it has been shown [16] that by effective characterization of the non-Markovian noise one can extend the coherence lifetime of multiqubit systems. This solidifies the need for a deeper understanding of many-bodied interactions with non-Markovian environments. Understanding these control mechanisms may lead to designing better and more robust technologies that have a plethora of implementations, including that of quantum networks [17] and clocks

*a.d.burgess@surrey.ac.uk
†m.florescu@surrey.ac.uk

[18]. Another difficulty facing quantum technologies, beyond the preservation of entanglement, is the generation of such entanglement. An interesting recent development shows that it is possible to utilize the non-Markovianity of the environment to generate entanglement between initially uncorrelated atomic systems [19,20]. By understanding the bidirectional flow of information between system and environment—the essence of non-Markovian systems—it becomes possible to transfer information, and therefore quantum correlations between systems using the environment as an intermediary. It is of great interest to be able to prepare and control these entangled states for quantum computation applications. Photonic band gap systems appear to be naturally suited for generating such interatomic entanglement, as the atoms couple strongly to a single photonic band edge mode [13] allowing for efficient energy transfer between atoms, even in the absence of direct dipole-dipole interactions.

In this work, we study the single-excitation regime of many-body two-level systems that interact dissipatively with generically structured bosonic reservoirs—that can be described by a continuum of quantum harmonic oscillators—and reveal some remarkable characteristics. We also apply the formalism developed for a model system, that of the isotropic photonic crystal, a particularly interesting example which displays what can be considered the highest degree of non-Markovianity for a reservoir due to the divergence in its density of states at the photonic band edge [14]. Such spin-coupled systems have been realized in a plethora of experiments, including quantum dots [21], superconducting networks [22], trapped ions [23], cold atoms inside of optical lattices [24], and more recently within photonic crystal wave guides [25–27].

Previous studies have considered the two-qubit interaction with independent reservoirs utilizing the second-order time-convolutionless approach [28], the study of entanglement of two qubits coupled to a single reservoir [29–31], the single-excitation dynamics for a single-spin in a non-Markovian reservoir [32], the single-excitation dynamics of two coupled atoms inside three-dimensional anisotropic photonic crystals [33], and the entanglement generation in N atom systems within the weak-coupling regime [20]. In this study we go further by studying the dynamics of N coupled atomic systems coupled—not necessarily weakly—to generic bosonic reservoirs that can be adequately described by a local density of states around the atomic system location. Such models are useful in understanding the induced dynamics of atomic systems in a range of environments such as the quantized electromagnetic fields as well as nonzero temperature vibronic environments.

This article is organized as follows. In Sec. II we employ the Schrödinger equation to study the single excitation dynamics of N coupled atomic systems embedded within a single bosonic reservoir. Two system topologies are considered, the first being symmetric coupling wherein all the atoms are coupled to one another with the same coupling strength and a nearest-neighbor system wherein atoms only interact with adjacent partners describing a chain of atoms. We study the late time behavior of the excited-state populations for each system. In Sec. III we contrast these results with those for independent reservoir dissipative systems. Finally, in Sec. IV we consider the specific case of the photonic crystal and derive the full time evolution for the system wherein the transition energies of the atoms are close to an isotropic photonic band gap—a model system that has very strong non-Markovian characteristics due to a divergence in the local density of states of the electromagnetic field around a photonic band gap. We then study the preservation and generation of entanglement between the N atoms in the system as well as how non-Markovianity is modulated with the number of atomic systems N.

II. MANY ATOMS IN A SINGLE BOSONIC RESERVOIR

We begin with a system of N two-level atoms embedded within a single structured reservoir, with all atoms coupling to the reservoir with the same coupling strengths. To facilitate analytic solutions we assume that the reservoir is initially in its vacuum state. Such assumptions are justified for very low-temperature systems. Furthermore, in the case of photonic crystals with a photonic band edge, energetic modes of the electromagnetic field with energy less than the band gap frequency ω_I are not accessible and as such cannot be excited by thermal fluctuations. For band-gap frequencies in the optical range, the thermal fluctuations exciting electromagnetic field modes with energy greater than the band gap are negligible [34,35]. Furthermore, we deploy the rotating wave approximation (RWA) to restrict our study to the single excitation sector of the Hilbert space.

A. Fully symmetric coupling

The first model we consider is a many-body dissipative system wherein the atomic systems are coupled to each other and the bosonic reservoir with the same coupling strengths. For such a model, there are two relevant length scales, the first being the spatial range of the interatomic coupling generated by the dipole-dipole interaction. The second is the total size of the atomic ensemble. We require the local density of states for the reservoir across both length scales to remain the same. However, it is clear that the length scale of the dipole-dipole interaction is necessarily smaller than the ensemble size and such models have been used to effectively describe superradiant effects in electromagnetic field reservoirs [36–38]. The Hamiltonian associated with this model in the rotating wave approximation is given by

$$H = \sum_{i=1}^{N} \omega_0 \sigma_i^+ \sigma_i^- + \sum_{\lambda} \omega_\lambda a_\lambda^\dagger a_\lambda + i \sum_{i,\lambda} g_\lambda (a_\lambda \sigma_i^+ - a_\lambda^\dagger \sigma_i^-) + \sum_{i \neq j} J \sigma_i^+ \sigma_j^-, \quad (1)$$

where σ_i^+ and σ_i^- are the excitation and deexcitation operators for the ith atomic system, respectively, a_λ and $a_\lambda^\dagger$ are the bosonic field annihilation and creation operators, ω_0 and ω_λ are the atomic transition and the λ-boson mode frequencies, g_λ is the coupling strength of the atomic system and the λ-boson mode [36,39,40], and J is the dipole-dipole coupling strength between atoms. This is equivalent to a Dicke model [38] for N atoms with a coupling between each of the atoms.

The Hamiltonian has the convenient property that it conserves the excitation number [41], that is to say it commutes with the number operator $N = \sum_{i=1}^{N} \sigma_i^+ \sigma_i^- + \sum_\lambda a_\lambda^\dagger a_\lambda$. As such we consider the single excitation wave function given by

$$\phi(0) = c_0\psi_0 + \sum_i^N c_i(0)\psi_i + \sum_\lambda c_\lambda(0)\psi_\lambda, \tag{2}$$

where $\psi_i = |i\rangle_A |0\rangle_B$ is the state wherein the ith atom is in its excited state and all other atoms and the reservoir are in the ground state. $\psi_\lambda = |0\rangle_A |\lambda\rangle_B$ represents all atoms in their ground state and the bosonic system has its λ mode excited. $\psi_0 = |0\rangle_A |0\rangle_B$ denotes the ground state of the entire system. The time evolution of this state is given by

$$\phi(t) = c_0\psi_0 + \sum_i^N c_i(t)\psi_i + \sum_\lambda c_\lambda(t)\psi_\lambda. \tag{3}$$

It is convenient to introduce the following parameter that sums over the excited-state amplitudes:

$$c_+(t) = \sum_{i=1}^{N} c_i(t). \tag{4}$$

The Schrödinger equation generates the set of coupled differential equations for the state amplitudes:

$$\begin{aligned}
\dot{c}_i &= -iJ(c_+ - c_i) + \sum_\lambda c_\lambda g_\lambda e^{i(\omega_0-\omega_\lambda)t}, \\
\dot{c}_+ &= -iJ(N-1)c_+ + N\sum_\lambda c_\lambda g_\lambda e^{i(\omega_0-\omega_\lambda)t}, \\
\dot{c}_\lambda &= -g_\lambda e^{-i(\omega_0-\omega_\lambda)t} c_+.
\end{aligned} \tag{5}$$

Assuming now that the bosonic field is initially in its vacuum configuration $[c_\lambda(0) = 0, \forall\lambda]$, formally integrating the differential equation for c_λ yields

$$c_\lambda(t) = -\int_0^t g_\lambda e^{-(\omega_0-\omega_\lambda)t_1} c_+(t_1)dt_1. \tag{6}$$

We introduce the so-called "memory kernel" $G(t) = \sum_\lambda g_\lambda^2 e^{i(\omega_0-\omega_\lambda)t}$. Substituting Eq. (6) in Eqs. (5) we obtain

$$\begin{aligned}
\dot{c}_i &= -iJ(c_+ - c_i) - \int_0^t G(t-t_1)c_+(t_1)dt_1, \\
\dot{c}_+ &= -iJ(N-1)c_+ - N\int_0^t G(t-t_1)c_+(t_1)dt_1.
\end{aligned} \tag{7}$$

Note that the dynamics induced by the bosonic reservoir are solely controlled by the value of c_+ convoluted with the memory kernel $G(t)$; this can be interpreted as the reservoir only coupling to the total polarization of the collection of atoms. To emphasize this point, we can consider the total polarization operator $\sigma_T^- = \sum_{i=1}^N \sigma_i^-$, which is the sum of the polarization for each of the atomic systems. The expectation value of this operator is $\langle\sigma_T^-\rangle = c_0 c_+(t) \propto c_+(t)$, suggesting that c_+ is a measure of the total system's polarization. Similarly, the atom-atom coupling term is $\propto c_+ - c_i$, so we can interpret this as the individual atom coupling to the total polarization of all the other atoms in the system. Additionally, it is this convolution term in Eq. (7) that controls the non-Markovianity of the system's dynamics as it integrates over all previous time states of the system, effectively allowing for previous states of the system to impact the current time dynamics. This is a truly non-Markovian process as the convolution accounts for states from the initial condition at $t = 0$ up to the current time t. The strength of the non-Markovianity of the system is then determined by the particular character of the memory kernel $G(t - t_1)$. This is clear when noting that for $G(t - t_1) = \delta(t - t_1)$ we have purely Markovian dynamics as the memory kernel only gives information when the two times are equal.

Equation (5) can be solved in terms of the Laplace transform of the single atom amplitudes c_i and c_+ (the full derivation is presented in Appendix A1). We obtain for the value of the total polarization c_+ of the atoms

$$\tilde{c}_+(s) = \frac{c_+(0)}{s + iJ(N-1) + N\tilde{G}(s)}, \tag{8}$$

where $\tilde{G}(s)$ is the Laplace transform of the memory kernel. It is often useful to think of the environmental modes being distributed in a continuum such that we can relate $\tilde{G}(s)$ to the spectral density $S(\omega)$—describing the coupling strengths of the atomic systems to the environment at different environmental frequencies defined by

$$S(\omega) = \sum_\lambda g_\lambda^2 \delta(\omega - \omega_\lambda). \tag{9}$$

Thus the relation between the Laplace transform of the memory kernel and the spectral density is

$$\tilde{G}(s) = \int d\omega \frac{S(\omega)}{s - i(\omega_0 - \omega)}. \tag{10}$$

Interestingly the dynamics associated with the total polarization parameter c_+ maps onto the single $(N = 1)$ atomic system

$$\tilde{c}_1(s) = \frac{c_1(0)}{s + \tilde{G}(s)}, \tag{11}$$

with rescaled coupling strengths $g_\lambda \to \sqrt{N} g_\lambda$ and a Lamb shift of the transition frequency $\omega_0 \to \omega_0 + J(N-1)$, which ultimately leads to a phase parameter $e^{iJ(N-1)t}$ in the time resolved dynamics. The Laplace transforms of the individual state amplitudes are given by

$$\tilde{c}_i(s) = \frac{c_i(0)}{s - iJ} - \frac{c_+(0)[\tilde{G}(s) + iJ]}{(s - iJ)[s + iJ(N-1) + N\tilde{G}(s)]}. \tag{12}$$

The Laplace transform solutions in Eqs. (11) and (12) provide a few interesting results. Note that the coupling to the reservoir dynamics is strongly dependent on the initial value of the total polarization $c_+(0)$. Also, note that we can decouple the atoms from their environment by choosing an appropriate initial condition such that the initial total polarization $c_+(0) = 0$. Doing so leaves only the first term on the right-hand side of Eq. (12) nonzero. The inverse Laplace transform of this leads to only time evolution in the phase of each excited-state amplitude $c_i(t) = c_i(0)e^{iJt}$ and does not affect population dynamics. This is because the total polarization for the system is zero, preventing the atoms from coupling to the

environment. Another initial condition of note is full initial symmetry, such that each atom has equivalent time evolution. Each atom acts identically towards the evolution of the total polarization and, as such, each acts as a single atom within a dissipative environment as the gain in excitation due to energy transfer between atoms is balanced with the loss. For example, assuming $c_i(0) = \frac{1}{\sqrt{N}}$ and $c_+(0) = \sqrt{N}$ the evolution of the excited-state amplitudes is governed by

$$\tilde{c}_i(s) = \frac{1}{\sqrt{N}[s + iJ(N-1) + N\tilde{G}(s)]}, \tag{13}$$

which is simply the rescaled dynamics of c_+ in Eq. (8).

We also find that the steady state of these systems is nonzero. The total polarization for the system tends to relax in a conventional sense; however, this does not necessitate that individual atoms relax back to the ground state as we only require the total polarization to relax. Using the final value theorem (FVT) and removing the phase dependence ($s \to s + iJ$) yields

$$c_{i\infty} = \lim_{s\to 0} s\tilde{c}_i(s + iJ) = c_i(0) - \frac{c_+(0)}{N}. \tag{14}$$

As such, we expect the late time excited-state population of the ith atom $|c_i|^2$ to tend towards $|c_i(0) - \frac{c_+(0)}{N}|^2$ discounting oscillations as the FVT does not account for these. Effectively, by configuring the initial condition of the atomic systems, we can localize excitations in particular atoms. Such a technique may have relevance in quantum memory storing devices.

An interesting case occurs when the total polarization for the atoms is equal to a single atom's polarization [$c_1(0) = c_+(0)$]. As the environment only couples to the total polarization and the relaxation of the total polarization is carried equally across all of the atomic systems this allows for nonzero steady-state polarizations for individual atoms even in highly dissipative or Markovian environments—where the total polarization goes to zero. This is apparent when we apply the final value theorem with this initial condition yielding $c_{1\infty} = c_1(0)(1 - \frac{1}{N})$. As we increase the number of atoms within the system we have $\lim_{N\to\infty} c_{1\infty} = c_1(0)$ so, in the late time, we return to our initial-state value (minus phase contributions). Scaling the numbers of atoms effectively increases the speed of the relaxation of the total polarization as its coupling to the reservoir $\sqrt{N}g_\lambda$ is dependent on N, so we can imagine that as N increases we get limited reservoir dynamics induced on the individual atoms as the changes in the total polarization are spread amongst all N atoms.

We now present an effective Hamiltonian model to show how the dynamics we are seeing are similar to that of a single atomic system with an altered effective Hamiltonian. To model this behavior we consider a single atomic system embedded within a bosonic reservoir with an additional self-interaction term to account for the atom-atom interactions. The system Hamiltonian is given by

$$\begin{aligned}\tilde{H} =& \omega_0\sigma^+\sigma^- + \sum_\lambda \omega_\lambda a_\lambda^\dagger a_\lambda + J(N-1)\sigma^+\sigma^- \\ &+ i\sqrt{N}\sum_\lambda g_\lambda(a_\lambda\sigma^+ e^{i(\omega_0-\omega_\lambda)t} - a_\lambda^\dagger\sigma^- e^{-i(\omega_0-\omega_\lambda)t}).\end{aligned} \tag{15}$$

We note that the coupling to the reservoir of this new aggregated atom is stronger (for $N > 1$) than in the original system. This leads to an interaction Hamiltonian of the form

$$\begin{aligned}\tilde{H}_I =& J(N-1)\sigma^+\sigma^- \\ &+ i\sqrt{N}\sum_\lambda g_\lambda(a_\lambda\sigma^+ e^{i(\omega_0-\omega_\lambda)t} - a_\lambda^\dagger\sigma^- e^{-i(\omega_0-\omega_\lambda)t}),\end{aligned} \tag{16}$$

and the dynamical equation for the excited-state amplitude c'_+ is given by

$$\dot{c}'_+ = -iJ(N-1)c'_+ + \sqrt{N}\sum_\lambda c_\lambda g_\lambda e^{i(\omega_0-\omega_\lambda)t}, \tag{17}$$

yielding

$$\dot{c}'_+ = -iJ(N-1)c'_+ - N\int_0^t G(t-t_1)c'_+(t_1)dt_1, \tag{18}$$

which is equivalent to Eq. (7). As such we can consider that the reservoir-atom interaction is being mediated by the aggregated system that has internal couplings that the reservoir cannot see.

Now we consider how altering the coupling J between the atoms impacts the steady-state dynamics. In the regime where $J \to 0$ the steady-state behavior—nonzero excited-state populations—still occurs, provided that

$$\lim_{s\to 0}\frac{\tilde{G}(s)}{s + N\tilde{G}(s)} \tag{19}$$

exists. To see this we can consider that the memory kernel in terms of the spectral density is g

$$\lim_{s\to 0^+}\tilde{G}(s) = \lim_{s\to 0^+}\int d\omega\frac{S(\omega)}{s - i(\omega_0 - \omega)}. \tag{20}$$

Utilizing the Sokhotski-Plemelj theorem [42] we obtain

$$\lim_{s\to 0^+}\tilde{G}(s) = S(\omega_0)\pi - i\mathrm{P}\int_0^\infty d\omega\frac{S(\omega)}{\omega - \omega_0}, \tag{21}$$

where P refers to the Cauchy principal value. As such, we expect the above to be generally nonzero and thus that we have nonzero steady-state values. For example, we consider a generic Ohmic type spectral density with Ohmicity parameter p given by

$$S(\omega) = \lambda\Omega\Big[\frac{\omega}{\Omega}\Big]^p e^{-\omega/\Omega}, \tag{22}$$

where λ is the coupling strength and Ω the cutoff frequency. We have

$$\begin{aligned}\lim_{s\to 0^+}\tilde{G}(s) =& S(\omega_0)\{\pi[1 + i\,\mathrm{Cot}(\pi p) - i(-1)^p\mathrm{Csc}(\pi p)] \\ &- i(-1)^p\Gamma(1+p)\Gamma(-p, -\omega_0/\Omega)\},\end{aligned} \tag{23}$$

where $\Gamma(\cdot)$ and $\Gamma(\cdot,\cdot)$ are the gamma and incomplete gamma functions, respectively. As this value of the Laplace transform for the memory kernel is nonzero we do not have issues in reducing out this term in finding the final value for the excited-state amplitudes. Thus reservoirs that can be modeled by the Ohmic types of spectral density would yield the steady states predicted by Eq. (14).

These results provide a solid basis for the current exploration of the non-Markovian dynamics as well as being amenable to our intuition that the dynamics are controlled by the total polarization of the system. However, it is often the case in real physical systems that such an exact symmetry is not attainable and that local defects in the structure of the environment will modulate the dipole-dipole coupling between the atomic systems. As such in Appendix A2 we have considered a single defect in the atomic dipole-dipole coupling. We note that the steady state from the FVT yields

$$c_i^{\infty} = c_i(0) + \frac{c_k(0) - c_+(0)}{N-1}.$$

The steady state of the system excludes the initial condition of the defect atom $c_k(0)$. This is quite remarkable that, despite the introduction of the defect, the only change at the steady state is the removal of that defect from the total polarization. Additionally, by studying the form of the Laplace space solutions for the excited-state amplitudes in Eq. (A20), we note that there are now three dynamical terms associated with the environment. The first is proportional to the polarization of the symmetric atoms [$\propto c_+(0) - c_k(0)$]. The second is proportional to the polarization of the defect atom [$\propto c_k(0)$]. Finally, there is a term proportional to the initial polarization of the entire system [$\propto c_+(0)$]. This means that for a preferentially selected initial condition we could again decouple the system from its environment. This is done by setting these initial polarizations to zero. Furthermore, we have provided a scheme in Appendix A3 for studying the case where the ith and jth atoms are coupled with a dipole-dipole interaction J_{ij}, accounting for generic dipole-dipole coupling. In principle, solving this equation is equivalent to inverting an affine transformation.

B. Nearest-neighbor coupling

In this section, we consider a different model for atomic systems in dissipative environments—that of an atomic chain, allowing the atoms to only interact directly with immediate neighboring atoms. We consider an open chain such that at the boundaries the first and Nth atoms couple only to the second and $(N-1)$th atoms, respectively. This model is much less restrictive in terms of the symmetry of the dipole-dipole coupling strength J as we need only to assume that atoms are equidistant from their nearest neighbors, although more care is needed in justifying coupling to the same reservoir, i.e., that the g_λ are shared across all atomic systems. However, note that dipole-dipole interactions occur over short length scales of less than 10 nm [43]; naturally we would not expect the electromagnetic field to vary greatly over this length scale justifying the identical coupling. Alternatively, if considering coupling to a photonic crystal reservoir, the atoms could be placed at spatially equivalent positions within the crystalline structure. The system Hamiltonian in the interaction picture is given by

$$\begin{aligned}\tilde{H}_I =& i\sum_{i,\lambda} g_\lambda (a_\lambda \sigma_i^+ e^{i(\omega_0-\omega_\lambda)t} - a_\lambda^\dagger \sigma_i^- e^{-i(\omega_0-\omega_\lambda)t}) \\ &+ \sum_{j=1}^{N-1} J(\sigma_j^+\sigma_{j+1}^- + \sigma_j^-\sigma_{j+1}^+),\end{aligned} \tag{24}$$

where we note that, as stated above, only the next-neighboring atoms are coupled to each other. By performing a similar analysis to the highly symmetric case and keeping only terms up to second order in the dipole-dipole coupling parameter J—as the dipole-dipole coupling is weak—we obtain the following equation for the excited-state amplitude of the first atom in the chain

$$\begin{aligned}\tilde{c}_1(s) =& \frac{s^2 c_1(0) - iJs c_2(0) - J^2 c_3(0)}{(s^2+J^2)s} \\ &+ \frac{\tilde{c}_+(s)\tilde{G}(s)(J^2 + iJs - s^2)}{(s^2+J^2)s}.\end{aligned} \tag{25}$$

We can derive a similar expression for the Laplace transform solution for the excited-state amplitude of the final atom in the chain:

$$\begin{aligned}\tilde{c}_N(s) =& \frac{s^2 c_N(0) - iJs c_{N-1}(0) - J^2 c_{N-2}(0)}{(s^2+J^2)s} \\ &+ \frac{\tilde{c}_+(s)\tilde{G}(s)(J^2 + iJs - s^2)}{(s^2+J^2)s}.\end{aligned} \tag{26}$$

Keeping terms up to second order in the dipole-dipole coupling J effectively allows for the dynamics of the nearest two atoms to intervene directly in the dynamics of the system. We note that the reservoir induced dynamics [terms proportional to $\tilde{G}(s)$] are again determined by the total polarization parameter c_+. However, as the atoms are only coupled to their nearest neighbors, we pick up additional contributions from the dipole-dipole coupling J.

In contrast to the fully symmetric case, we now pick up oscillatory terms given by the initial conditions of each of the two nearest atoms as shown by the terms independent of $\tilde{G}(s)$ (these are simple Laplace transform identities for integrals of the trigonometric sin and cos functions). This demonstrates the clear bidirectionality of the energy transfer that was not present in the previous model.

For convenience we now consider the expansion up to first order in J and assume only that the first atom is initially excited, $c_1(0) = 1$, and all other atoms are initially in the ground state, $c_i(0) = 0$. This yields

$$\begin{aligned}\tilde{c}_1(s) &= \frac{1}{s} - \frac{\tilde{G}(s)}{[s^2 + N\tilde{G}(s)s - 2iJ\tilde{G}(s) + 2iJs]} \\ \tilde{c}_N(s) &= -\frac{\tilde{G}(s)}{[s^2 + N\tilde{G}(s)s - 2iJ\tilde{G}(s) + 2iJs]}.\end{aligned} \tag{27}$$

In order to explore the late time dynamics, we consider the transformation $s \to s + \frac{2iJ}{N}$. Up to first order in the dipole-dipole coupling J, we have

$$c_1(\infty) = 1 - \frac{\tilde{G}\left(\frac{2iJ}{N}\right)}{2iJ\left(1+\frac{2}{N}\right) + N\tilde{G}\left(\frac{2iJ}{N}\right)}. \tag{28}$$

Unlike the fully symmetric case explored previously, the late time dynamics appear to be governed by the value of $\tilde{G}(\frac{2iJ}{N})$. However, for large values of $\tilde{G}(\frac{2iJ}{N})$ or large values of N and with $\tilde{G}(\frac{2iJ}{N}) \neq 0$ we recover similar dynamics to the fully symmetric system presented above. Conversely, for smaller values of N we find that the steady-state character is strongly determined by the relation between the dipole-dipole coupling

strength J and the memory kernel $\tilde{G}(s)$. In Appendix A5, we show that even for small perturbations of the transition energy in the first and final atom in the chain we recover the same dynamics with a phase shift and frequency shift in these modified atoms' amplitudes. Such a correction shows that for small perturbations in these transition energies we can retain the dynamics of the combined system ensuring the system is robust.

This model could also be utilized to study quantum chaotic chains, as one would need only to add an Ising interaction coupling term (σ^z) between the atoms and a modulated transition energy in a single atom in the chain to induce quantum chaos (see Refs. [44,45]). Fortunately, such coupling terms ($\sigma_i^z\sigma_{i+1}^z$) also commute with the number operator and thus conserve the number of excitations in the system allowing for the formalism developed here to be utilized directly. This opens the possibility to deploy the current framework to explore the effects of a quantum chaotic chain within a dissipative environment.

III. MANY ATOMS IN SEPARATE BOSONIC RESERVOIRS

Here we consider the case wherein each of the atoms are coupled to independent bosonic reservoirs. This model assumes that the local environment between atomic systems has varied sufficiently such that there are no correlations between the local environments of different atoms. Similar models are utilized in quantum chemistry to model the energy transfer in light-harvesting complexes [46], and we explore it here in our formalism merely to contrast it with the single reservoir case.

A. Fully symmetric coupling

For independent reservoirs interacting with each of the atoms we need to introduce separate creation and annihilation operators for the different reservoirs. The interaction Hamiltonian in the Dirac picture in this regime then becomes

$$\tilde{H}_I = i\sum_{i\lambda} g_\lambda (a_{i\lambda}\sigma_{i+}e^{i(\omega_0-\omega_\lambda)t} - a_{i\lambda}^\dagger\sigma_{i-}e^{-i(\omega_0-\omega_\lambda)t}) + \sum_{j\neq i} J\sigma_i^+\sigma_j^-, \tag{29}$$

where we have an additional index on the annihilation and creation operators for the bosonic reservoir to denote each of the independent reservoirs associated to each atom. This leads to the Laplace transform of the excited state populations $\tilde{c}_i(s)$:

$$\tilde{c}_i(s) = \frac{c_i(0)}{s - iJ + \tilde{G}(s)} - \frac{iJc_+(0)}{[s + iJ(N-1) + \tilde{G}(s)][s - iJ + \tilde{G}(s)]}. \tag{30}$$

In contrast to the previous section here we note that, while there is a collective effect governed by the total polarization c_+, we have also a decaying in the individual systems governed by $c_i(0)$. This behavior is apparent from the fact that we can transform the first term into the single atom dynamics by way of taking $s \to s + iJ$ (simply introducing a phase parameter in the time domain), effectively shifting the transition energy of the atomic system by J. Furthermore, we note that the denominator for the term associated with the total polarization no longer has a $N\tilde{G}(s)$ term, showing that superradiant effects no longer play a role as the effective coupling strength no longer scales with the number of atoms. If we utilize the final value theorem as before we can see that, even with the removal of the phase parameter e^{iJt}, the amplitudes vanish in steady-state conditions due to the nonzero nature of the Laplace transform of the memory kernel:

$$\lim_{s\to\infty} s\tilde{c}_i(s) = 0. \tag{31}$$

As such we no longer observe the steady-state character we saw in the previous section. We can also note that the collective dynamics is a convolution of two systems undergoing decay into a reservoir as we now have multiple pathways for the excitation to leave the system and if the excitation enters another atom's reservoir it is now much more difficult for it to be retrieved by the other atoms; whereas previously all of the atoms may take the excitation from the same unique reservoir, now only one atom may do so, which is that corresponding to the reservoir the excitation is in.

B. Nearest-neighbor coupling

Similar to the previous section we now consider the system wherein the atoms can only couple to adjacent atoms in a line. For this system the appropriate interaction Hamiltonian is given by

$$\tilde{H}_I = i\sum_{i,\lambda} g_{i\lambda}(a_{i\lambda}\sigma_i^+ e^{i(\omega_0-\omega_{i\lambda})t} - a_{i\lambda}^\dagger\sigma_i^- e^{-i(\omega_0-\omega_{i\lambda})t}) + \sum_{j=1}^{N-1} J(\sigma_j^+\sigma_{j+1}^- + \sigma_j^-\sigma_{j+1}^+). \tag{32}$$

Similar to the previous approach, we can evaluate the Laplace transform of the excited-state amplitudes for the central atoms in the chain, i.e., for $\tilde{c}_i$, $i \neq 1, N$,

$$\tilde{c}_i(s) = \frac{c_i(0)[s + \tilde{G}(s)] - iJ[c_{i-1}(0) + c_{i+1}(0)]}{[s + \tilde{G}(s)]^2 + 2J^2} + \frac{J^2[c_{i-2}(0) + c_{i+2}(0)]}{[s + \tilde{G}(s)]\{[s + \tilde{G}(s)]^2 + 2J^2\}}, \tag{33}$$

for $i \neq 1, N$ which leads to the Laplace solutions for the first and final atom in the chain

$$\tilde{c}_{1,N} = \frac{c_{1,N}(0)}{s + \tilde{G}(s)} - \frac{iJ\tilde{c}_i(s)}{s + \tilde{G}(s)}. \tag{34}$$

Note that all terms contain the Laplace transform of the memory kernel $\tilde{G}(s)$ in the denominator; as such we expect them each to decay away into the reservoir and that there is not any observable shielding of these amplitudes. Again, utilizing the final value theorem we find that—typically—we do not have nonzero steady states. Thus it is apparent that to maintain these nonzero steady states irrespective of the specific form of the memory kernel we must ensure that the atomic systems are all coupled to the same local reservoir. This is akin to stating that these atomic systems need to be highly localized.

IV. PHOTONIC CRYSTAL RESERVOIR

In this section, we consider a specific model for the bosonic reservoir, that of the electromagnetic field around the photonic band gap of a photonic crystal. The photonic crystal is well suited for the model proposed as due to its screening of modes of the electromagnetic fields the low-temperature approximation is well justified. Additionally, as photonic crystals can have band-gap frequencies in the optical spectral range, the rotating wave approximation is also well justified. Furthermore, experimental setups [25,27] have already been developed for studying atomic systems embedded within photonic crystals and, as such, we can validate our approach against experimental data. The photonic crystal also has the additional useful quality that as we increase the dephasing value Δ (the difference between the atomic transition energy ω_0 and the photonic band edge ω_I) to large positive values we effectively see an unstructured vacuum and for large negatives values we see little of the electromagnetic field modes making the atoms act as free (no reservoir) coupled atoms. Thus, by varying the dephasing, we can inspect a variety of different environment configurations and regimes to properly test our models. The model for the photonic crystal we have chosen is that of the isotropic one-dimensional photonic crystal band edge [15,47]. Such a system can be constructed in the form of a photonic crystal waveguide [48]. This model is particularly interesting due to a divergence in the local density of states of the electromagnetic field modes around the band edge frequency ω_I [$\rho(\omega) \propto \theta(\omega - \omega_I)(\omega - \omega_I)^{-\frac{1}{2}}$], generating strong atom-photon coupling and leading to localization of photons around atoms.

A. Fully symmetric coupling

To perform our analysis we need only derive the memory kernel for the isotropic band-gap model and then perform the inverse Laplace transforms required.

In Appendix C1, we have derived the excited-state amplitude for a memory kernel defining a photonic crystal band-gap material. Such a memory kernel has the form

$$\tilde{G}(s) = \beta^{3/2} e^{-i\pi/4} (s - i\Delta)^{-\frac{1}{2}}. \tag{35}$$

Note that this has a divergence at $s = i\Delta$; this is a direct consequence of the strong coupling to the band-gap mode of the local electromagnetic field. For convenience, we will assume that $\beta = 1$ and use the dimensionless time parameter $\tau = \beta t$.

From Eq. (C4) we note that if we remove the dipole-dipole coupling by taking $J \to 0$ then the exponential relaxation of the system has a decay rate $\gamma \propto N^{\frac{2}{3}}$, which reproduces the result found in [36] for uncoupled atomic systems inside a 1D photonic crystal, thus demonstrating superradiant behavior even in the single-excitation regime. Conversely, if we consider nonzero values for the dipole-dipole coupling J, then for large numbers of atomic systems N or small values of the dephasing Δ, we find that the decay rate $\gamma \propto N$ effectively increases the rate of superradiance by introducing dipole-dipole coupling. Remarkably this relationship has been observed for trapped atoms inside of 1D photonic waveguides where the decay rate was found to be proportional to the number of atoms N [49], hence validating our approach.

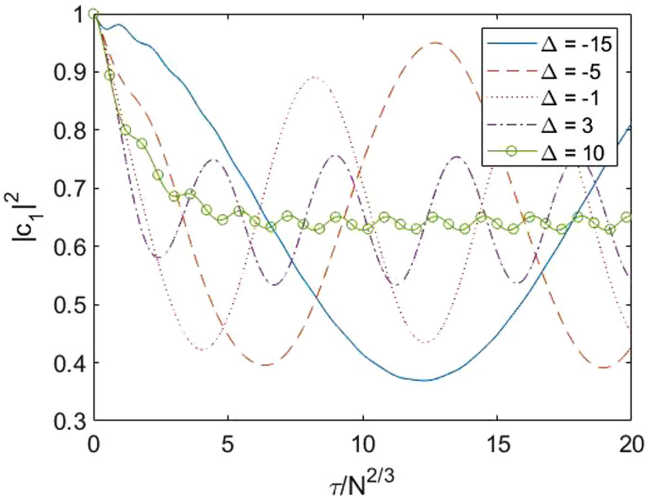

FIG. 1. Population dynamics for the excited state of a single atom coupled to four other atoms, with the atom initially excited [$c_1(0) = 1$], inside of a photonic crystal reservoir, with varying values of the dephasing parameter $\Delta = \omega_0 - \omega_I$ between the atomic transition energy and the photonic crystal band edge; the dipole-dipole coupling $J = 0.1$.

Resolving the time evolution of the system in Figs. 1, 2, and 3 (here atom 1 is initially excited), we note the predicted steady-state values (minus oscillations) of $1/N^2$ are present. As we increase the value of the dephasing Δ, we move closer to a vacuum state and so would traditionally expect the atoms to deexcite into the ground state. Additionally, due to the nature of the photonic crystal, we have nonzero steady states associated with the total polarization (acting as the

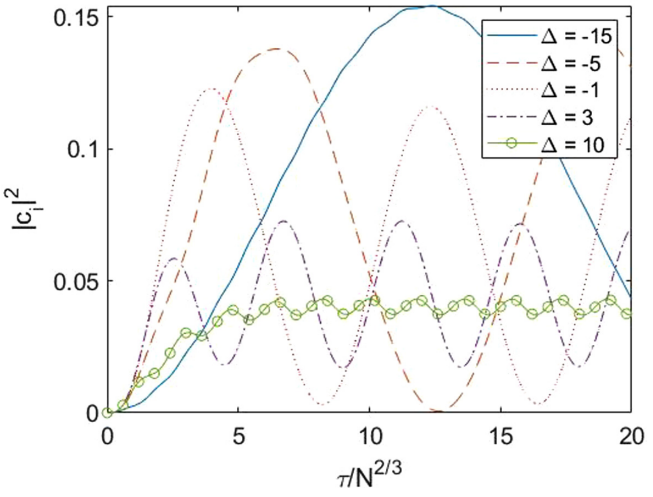

FIG. 2. Population dynamics for the excited state of a single atom coupled to four other atoms, with another atom initially excited [$c_1(0) = 1, i \neq 1$], inside of a photonic crystal reservoir, with varying values of the dephasing parameter $\Delta = \omega_0 - \omega_I$ between the atomic transition energy and the photonic crystal band edge; the dipole-dipole coupling $J = 0.1$.

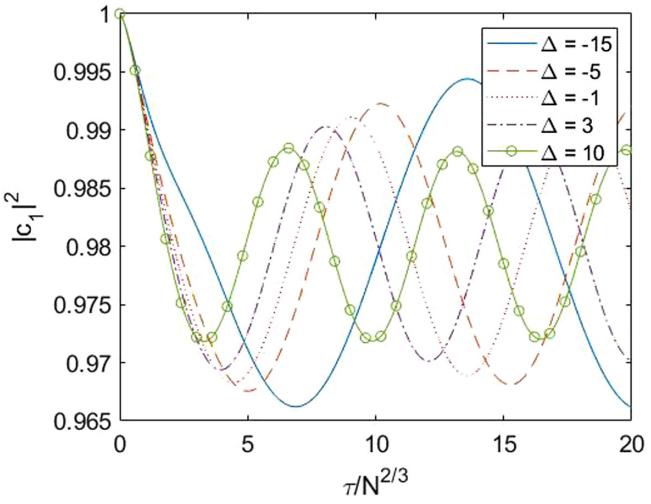

FIG. 3. Population dynamics for the excited state of a single atom coupled to 99 other atoms, with the atom initially excited $[c_1(0) = 1]$, inside of a photonic crystal reservoir, with varying values of the dephasing parameter $\Delta = \omega_0 - \omega_I$ between the atomic transition energy and the photonic crystal band edge; the dipole-dipole coupling $J = 0.1$.

single atom system from [13]) of the system. As such, we still have oscillations as the excitation is transferred between the different atoms. These amplitudes become damped as we increase the dephasing value, due to a monotonic reduction in the total polarization in Δ, or, equivalently, the increased dephasing makes it more difficult to transfer excitations to the band-gap mode. We also note that in Fig. 3 as the number of atoms increases the atoms move closer and closer in phase as $\Delta + J(N-1) \to JN$.

Figure 4 shows that, when the excited-state amplitudes for all atoms are initially prepared in a symmetrical excited

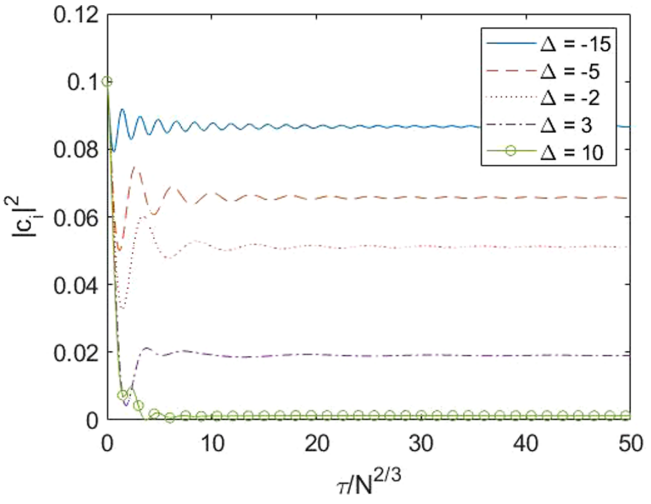

FIG. 4. Population dynamics for the excited state of a single atom coupled to nine other atoms, with all atoms symmetrically initially prepared $[c_i(0) = 1/\sqrt{10}]$, inside of a photonic crystal reservoir, with varying values of the dephasing parameter $\Delta = \omega_0 - \omega_I$ between the atomic transition energy and the photonic crystal band edge; the dipole-dipole coupling $J = 0.1$.

state $[c_i(0) = 1/\sqrt{10}$ for all $i]$, we return to the single atom $(N = 1, J = 0)$ excited-state amplitude's dynamics multiplied by $1/N$ with a Lamb shifted transition energy given by

$$\Delta \to \frac{\Delta + J(N-1)}{N^{2/3}}, \tag{36}$$

as predicted. As such we no longer see any transfer of excitations between respective atoms as each atom loses as much polarization as it gains from the other atoms in the system reaching an equilibrium. Additionally, as we increase the number of atoms N we effectively shift the atoms outside of the band gap as

$$N \gg \Delta/J, \kappa = \frac{\Delta + J(N-1)}{N^{2/3}} \to JN^{1/3}. \tag{37}$$

Next, we analyze the coherences between the energy eigenstates of the atomic systems. This is done by exploring the dynamics of the canonical Bell states. Typically, the environment causes decoherence in quantum systems. If we could identify environments that better preserve the coherences in atomic systems we may be able to engineer more robust quantum computing systems. The pair of Bell states accessible in this regime are

$$\Psi_+ = \frac{1}{\sqrt{2}}(|0\rangle|1\rangle + |1\rangle|0\rangle),$$
$$\Psi_- = \frac{1}{\sqrt{2}}(|0\rangle|1\rangle - |1\rangle|0\rangle). \tag{38}$$

If we consider a system of N atoms and we consider only two such atoms, we may choose to prepare the system in such a way that the two atoms have initial amplitudes $c_1(0) = \pm\frac{1}{\sqrt{2}}$ and $c_2(0) = \frac{1}{\sqrt{2}}$ such that the atoms are initialized in either of the two Bell states and the other $N-2$ atoms and environment in the ground state (with respect to their free Hamiltonians). From Eq. (C3) we can see that for the Ψ_- state—as the total initial polarization $c_+(0) = c_1(0) + c_2(0) = 0$—the system is decoupled from its environment and is well conserved. However, for the initial condition such that the two atoms are in the Ψ_+ state $c_+(0) = \sqrt{2}$, and thus we expect nontrivial reservoir induced dynamics. Although, as previously discussed, by increasing the number of atoms in the system we can reduce the effects of the reservoir on individual atoms. From Fig. 5 note that as we increase the number of atoms N in the system the amplitude of the oscillations away from the initial condition of the system is reduced, suggesting that increased auxiliary atoms may provide better conservation of the Bell state of the two atom system.

In addition to being able to preserve the entanglement between two atomic systems, we are also considering the generation of entanglement between atomic systems that are initially unentangled. It has been shown that non-Markovian bidirectional flow of information from system to the environment can generate entanglement between previously unentangled states [19,20], thus generating quantum correlations between atoms. The photonic crystal band-gap system is a natural candidate for this interaction as strong coupling to the band-gap mode between all of the atomic systems will effectively accommodate the transfer of information between atomic systems, even when the interatomic coupling $J = 0$,

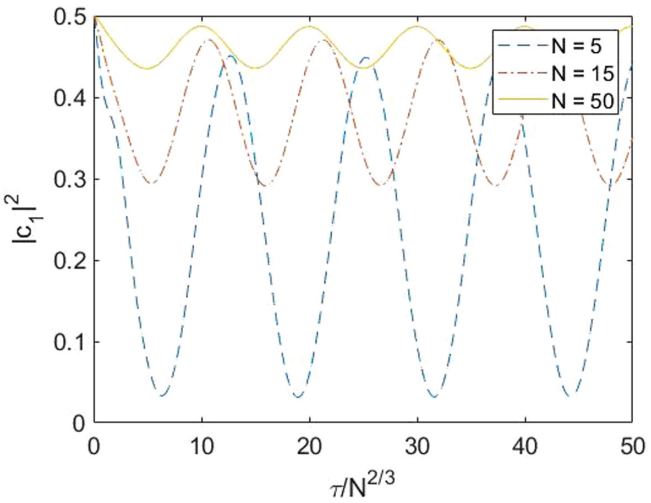

FIG. 5. Dynamics of the Bell state Ψ_+ for varying numbers of atoms N with value of the dephasing parameter $\Delta = \omega_0 - \omega_I = -5$ between the atomic transition energy and the photonic crystal band edge.

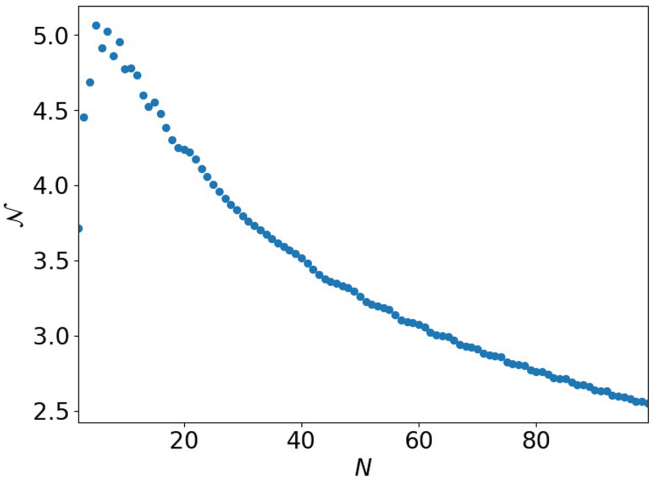

FIG. 7. Non-Markovian measure $\mathcal{N}$ against the number of atoms N in a photonic crystal, with transition energy of the atomic systems close to the band gap such that the dephasing with respect to the band edge frequency is $\Delta = -5$. The dipole-dipole coupling between atoms is $J = 0$.

hence generating quantum correlations associated with the entanglement. This stark backflow of information is characteristic of the non-Markovian nature of the photonic band-gap system.

The results presented in Fig. 6 show that this is the case. The concurrence between the initially excited atom and the other atoms in the system is nonzero even into the late-time dynamics, hence demonstrating the spontaneous generation of entanglement between the subsystems, which is mediated exclusively by the highly structured local electromagnetic field. Furthermore, the strength of the entanglement (the magnitude of the concurrence) is suppressed as we increase the number of atoms within our system. This is to be expected as we are considering only the single-excitation regime and, as the atom

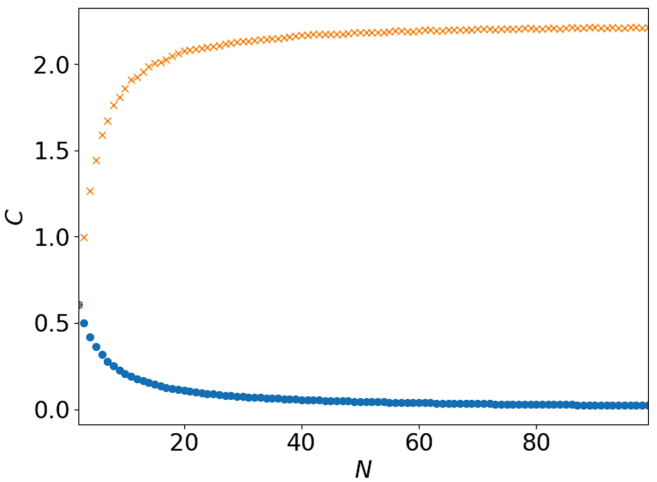

FIG. 6. Mean value of late-time concurrence C of atom 1 and atom $i \neq 1$ (blue circles) and total concurrence $(N-1)C$ (orange crosses) in a photonic crystal where the excitation is initially localized in atom 1 against the number of atoms in the system. The dipole-dipole coupling $J = 0$ and dephasing is $\Delta = -5$.

becomes less localized around the initially excited atom, we naturally expect a decrease in the localization in each other atom that is limited by the number of atoms. However, we note that this decays at a rate slower than $\frac{1}{N}$ and so, although the entanglement between pairwise atoms is lowered, the total entanglement of atom 1 and all others increases with atom number.

To justify whether this observed effect is due to the non-Markovianity in the system we need a way to quantify non-Markovianity. We utilize the metric introduced in [50], and consider the two trajectories to be the ground state and the time evolution of the reduced dynamics with atom 1 initially excited, to capture the system used in the generation of entanglement. Utilizing this metric we have studied the non-Markovianity in our system, the results of which are shown in Fig. 7. It is clear to see that the non-Markovianity reaches a maximum value around $N = 8$ atoms; this is a surprising fact as one would expect that the non-Markovianity would increase with the number of auxiliary atoms that atom 1 couples to. However, if we return to our previous analysis of the effective Lamb shift induced by increasing the number of atoms, the influence of the factors driving the dynamics of the system becomes clear. There is a discord between the non-Markovianity induced by the additional atoms that are resonant with atom 1 and with the Lamb shifting of the atomic frequency outside of the photonic band gap, the latter of which will lead to a more Markovian dynamics. As we increase the number of atoms, this Lamb shifting dominates and causes the system to appear more Markovian. Thus the apparent plateau in Fig. 6 can be associated with the reduction of the non-Markovianity of the system.

B. Nearest-neighbor coupling

We now consider the nearest neighbor coupling of a chain of atoms embedded within a photonic crystal. Similar to the previous approach we derive the excited-state amplitudes in

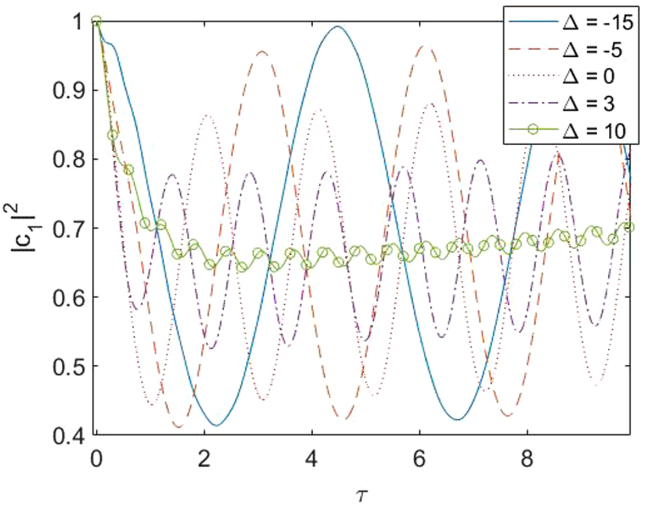

FIG. 8. Population dynamics for the excited state of the first atom in a chain of five atoms coupled to their nearest neighbor, with the first atom initially excited $[c_1(0) = 1]$, inside of a photonic crystal reservoir, with varying values of the dephasing parameter $\Delta = \omega_0 - \omega_I$ between the atomic transition energy and the photonic crystal band edge; the dipole-dipole coupling $J = 0.1$.

Appendix C2. For the dynamics of the first atom in the chains' excited-state amplitude we have

$$c_1(\tau) = c_1(0) + c_N(\tau). \tag{39}$$

Figures 8 and 9 depict the dynamics of the excited-state population of the first and fifth atom in a five-atom chain and we note that the results for this nearest-neighbor configuration are very similar to the dynamics of the fully coupled system. It becomes advantageous to explore as much as possible the fully coupled system, which has analytical solutions and extrapolate the results to the nearest-neighbor coupled system.

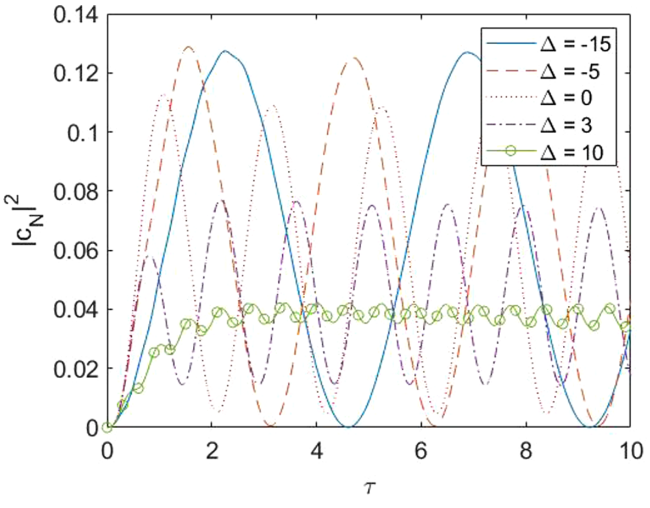

FIG. 9. Population dynamics for the excited state of the final atom in a chain of five atoms coupled to their nearest neighbor, with the first atom in the chain initially excited $[c_1(0) = 1]$, inside of a photonic crystal reservoir, with varying values of the dephasing parameter $\Delta = \omega_0 - \omega_I$ between the atomic transition energy and the photonic crystal band edge; the dipole-dipole coupling $J = 0.1$.

This behavior also suggests that the dynamics of the atomic system is being more significantly driven by the reservoir than the dipole-dipole coupling.

V. CONCLUSION

In this article, we have analyzed many-body atomic systems coupled to non-Markovian reservoirs and explored the emergent features. We have shown that the dynamics of symmetrically coupled atomic systems is controlled by the total polarizations of all atomic systems not uniquely by each. We have also studied the steady-state character of the atomic dynamics and have shown that it is determined by the number of atoms within the system. This effect was also shown to be independent of the specific structure of the reservoir the atoms are interacting with as well as the interatom dipole-dipole coupling strengths. We further expanded our analysis to the case of nearest-neighbor coupling between atoms to model an atomic chain and identified a similar steady state, that was less trivially determined by the dipole-dipole coupling. This is in contrast to coupling to independent reservoirs, wherein no such steady state can, in general, be achieved; this is due to there being multiple channels for the system to dissipate into without retrieval. Finally, we have explored the isotropic photonic band-gap model and have shown that it is possible to observe both the late time dynamics predicted as well as superradiant behavior. This superradiance can be enhanced by the dipole-dipole coupling between the atomic systems and both reproduced previous theoretical results, in the absence of dipole-dipole coupling, as well as found agreement with experimental results when reintroducing the dipole-dipole coupling [49], suggesting the necessity of this interaction in understanding the physical system. Our results demonstrate the viability of the approach introduced and suggest that such models may have physical constructions that could be of practical interest as they can effectively manipulate the localization of excitations across atoms simply by having more atoms supporting them [25]. Furthermore, we have shown that in this paradigm the single excitation Bell states $\Psi_\pm$ can be well preserved—a result that may prove useful for quantum computational systems. The generation of entanglement between atomic systems was explored by utilizing the photonic reservoir as an intermediary to transfer quantum correlations and we have shown that global entanglement increased with atomic number, suggesting a possible mechanism for preparing systems in entangled states. Finally, we studied the non-Markovianity of the system with a varying number of atoms and noticed a stark conflict between the influence of the Lamb shifting of the atomic transition frequency and the total number of atoms.

The data underlying the findings of this study are available without restriction [51].

ACKNOWLEDGMENTS

This work was supported by the Leverhulme Quantum Biology Doctoral Training Centre at the University of Surrey funded by a Leverhulme Trust training center Grant No. DS-2017-079 and the EPSRC (United Kingdom) Strategic

Equipment Grants No. EP/L02263X/1 (No. EP/M008576/1) and EPSRC (United Kingdom) Grant No. EP/M027791/1 awards to M.F. We acknowledge helpful discussions with the members of the Leverhulme Quantum Biology Doctoral Training Centre.

APPENDIX A: SINGLE RESERVOIR

1. Fully symmetric coupling

We start with the (RWA) Hamiltonian

$$H = \sum_{i=1}^{N} \omega_0 \sigma_i^+ \sigma_i^- + \sum_{\lambda} \omega_\lambda a_\lambda^\dagger a_\lambda + i \sum_{i,\lambda} g_\lambda (a_\lambda \sigma_i^+ - a_\lambda^\dagger \sigma_i^-) + \sum_{i \neq j} J \sigma_i^+ \sigma_j^-, \tag{A1}$$

where $\sigma_i^+$and σ_i^- are the excitation and deexcitation operators for the ith atomic system, respectively, a_λ and $a_\lambda^\dagger$ are the bosonic field annihilation and creation operators, ω_0 and ω_λ are the atomic transition and the λ-boson mode frequencies, and g_λ is the coupling strength of the atomic system and the λ-boson mode.

By changing to the interacting picture we can consider the interaction Hamiltonian

$$\tilde{H}_I = i \sum_{i,\lambda} g_\lambda (a_\lambda \sigma_i^+ e^{i(\omega_0-\omega_\lambda)t} - a_\lambda^\dagger \sigma_i^- e^{-i(\omega_0-\omega_\lambda)t}) + \sum_{j \neq k} J \sigma_j^+ \sigma_k^-. \tag{A2}$$

Such a Hamiltonian is convenient as it conserves the excitation number of any wave function. As such if we consider the single excitation wave function given by

$$\phi(0) = c_0 \psi_0 + \sum_{i}^{N} c_i(0) \psi_i + \sum_{\lambda} c_\lambda(0) \psi_\lambda, \tag{A3}$$

its time evolution is given by

$$\phi(t) = c_0 \psi_0 + \sum_{i}^{N} c_i(t) \psi_i + \sum_{\lambda} c_\lambda(t) \psi_\lambda, \tag{A4}$$

where for $\psi_i = |i\rangle_A |0\rangle_B$ the ith atom is in its excited state and $\psi_\lambda = |0\rangle_A |\lambda\rangle_B$ the atoms are all in their ground state and the bosonic system has its λ mode excited. By simply plugging this into the Schrödinger equation and determining the coupled differential equations of motion for the state amplitudes we get

$$\tilde{H}_I \phi_i = -i \sum_{\lambda} g_\lambda \psi_\lambda e^{-i(\omega_0-\omega_\lambda)t} + \sum_{j}^{N} J \psi_j (1 - \delta_{ij}), \tag{A5}$$

$$\tilde{H}_I \phi_\lambda = i g_\lambda e^{i(\omega_0-\omega_\lambda)t} \sum_{i} \psi_i. \tag{A6}$$

By introducing the parameter

$$c_+(t) = \sum_{i} c_i(t), \tag{A7}$$

we have

$$\begin{aligned} \dot{c}_i &= -iJ(c_+ - c_i) + \sum_{\lambda} c_\lambda g_\lambda e^{i(\omega_0-\omega_\lambda)t}, \\ \dot{c}_+ &= -iJ(N-1)c_+ + N \sum_{\lambda} c_\lambda g_\lambda e^{i(\omega_0-\omega_\lambda)t}, \\ \dot{c}_\lambda &= -g_\lambda e^{-i(\omega_0-\omega_\lambda)t} c_+. \end{aligned} \tag{A8}$$

Assuming the bosonic field is initially in its vacuum configuration $[c_\lambda(0) = 0]$ we can formally integrate up the last equation to get

$$c_\lambda(t) = -\int_0^t g_\lambda e^{-(\omega_0-\omega_\lambda)t_1} c_+(t_1) dt_1, \tag{A9}$$

and by introducing the memory kernel $G(t) = \sum_\lambda g_\lambda^2 e^{i(\omega_0-\omega_\lambda)t}$ we can rewrite the above equations as

$$\begin{aligned} \dot{c}_i &= -iJ(c_+ - c_i) - \int_0^t G(t-t_1) c_+(t_1) dt_1, \\ \dot{c}_+ &= -iJ(N-1)c_+ - N \int_0^t G(t-t_1) c_+(t_1) dt_1. \end{aligned} \tag{A10}$$

It is notable that our memory kernel $G(t)$ is related to the spectral density $S(\omega) = \sum_\lambda g_\lambda^2 \delta(\omega - \omega_\lambda)$ associated to the reservoir by the relation

$$G(t) = \int d\omega \, S(\omega) e^{i(\omega_0-\omega)t}. \tag{A11}$$

In order to solve these equations we utilize the Laplace transform. Transforming the differential equations into algebraic ones,

$$\begin{aligned} s\tilde{c}_i(s) - c_i(0) &= -iJ[\tilde{c}_+(s) - \tilde{c}_i(s)] - \tilde{c}_+(s)\tilde{G}_1, \\ s\tilde{c}_+(s) - c_+(0) &= -iJ(N-1)\tilde{c}_+(s) - N\tilde{c}_+(s)\tilde{G}_1, \end{aligned} \tag{A12}$$

where we have used that $\tilde{f}(s) = \mathcal{L}\{f(t)\}$. We can see that we can solve for $\tilde{c}_+(s)$ getting

$$\tilde{c}_+(s) = \frac{c_+(0)}{s + iJ(N-1) + N\tilde{G}}. \tag{A13}$$

From this we can solve for the single atom amplitude Laplace solution

$$\tilde{c}_i(s) = \frac{c_i(0)}{s - iJ} - \frac{c_+(0)(\tilde{G} + iJ)}{(s - iJ)[s + iJ(N-1) + N\tilde{G}]}. \tag{A14}$$

If we consider the form of $\tilde{G}(s)$ with respect to the spectral density we can see that

$$\tilde{G}(s) = \int d\omega \frac{S(\omega)}{s - i(\omega_0 - \omega)}. \tag{A15}$$

2. Single defect

For a fully symmetrically coupled system with a single defect at the kth atom, the atom has interspin coupling $J + \delta$ with all other atoms.

The interaction Hamiltonian associated with this system is given by

$$\tilde{H}_I = i\sum_{i,\lambda} g_\lambda (a_\lambda \sigma_i^+ e^{i(\omega_0-\omega_\lambda)t} - a_\lambda^\dagger \sigma_i^- e^{-i(\omega_0-\omega_\lambda)t}) + \sum_{j\neq l} J\sigma_j^+\sigma_l^- + \sum_{j\neq k}\delta(\sigma_j^+\sigma_k^- + \sigma_k^+\sigma_j^-). \quad \text{(A16)}$$

We have the Schrödinger equation evolution for the state amplitudes given by

$$s\tilde{c}_i = c_i(0) - iJ[\tilde{c}_+(s) - \tilde{c}_i] - i\delta\tilde{c}_k - \tilde{G}\tilde{c}_+, \quad \text{(A17)}$$

$$s\tilde{c}_k = c_i(0) - i(J+\delta)[\tilde{c}_+(s) - \tilde{c}_k] - \tilde{G}\tilde{c}_+, \quad \text{(A18)}$$

$$s\tilde{c}_+ = c_+(0) - i[(N-1)J+\delta]\tilde{c}_+ - (N-2)\delta\tilde{c}_k - \tilde{G}\tilde{c}_+. \quad \text{(A19)}$$

We can solve the algebraic equations above to solve for the Laplace transform solutions for the excited-state amplitudes given by

$$\tilde{c}_i(s) = \frac{1}{N-1}\left(\frac{c_i(0)(N-1)+c_k(0)-c_+(0)}{s-iJ} + \frac{s[c_+(0)-c_k(0)] + ic_k(0)[-N(\delta-i\tilde{G}+J)+\delta+J] + c_+(0)\tilde{G}}{\delta^2(N-1)+2\delta(N-1)(J-i\tilde{G})+(J+is)[J(N-1)-i(\tilde{G}N+s)]}\right), \quad \text{(A20)}$$

$$\tilde{c}_k(s) = \frac{c_k(0)\{i[\delta+J(N-1)]+\tilde{G}N+s\} - c_+(0)[\tilde{G}+i(\delta+J)]}{[s-i(\delta+J)]\{i[\delta+J(N-1)]+\tilde{G}N+s\} - i\delta(N-2)(i\delta+\tilde{G}+iJ)}, \quad \text{(A21)}$$

$$\tilde{c}_+(s) = -\frac{i[c_k(0)\delta(N-2)+c_+(0)(\delta+J+is)]}{\delta^2(N-1)+2\delta(N-1)(J-i\tilde{G})+(s-iJ)[iJ(N-1)+(\tilde{G}N+s)]}. \quad \text{(A22)}$$

By utilizing the final value theorem as before by taking $\lim_{s\to iJ}(s-iJ)\tilde{c}_i(s)$ we gain

$$c_i^\infty = c_i(0) + \frac{c_k(0)-c_+(0)}{N-1}. \quad \text{(A23)}$$

From this we can see that the defect mode reduces the steady-state contribution from the total polarization and in fact this term is entirely governed by the total symmetric part of the polarization $c_+ - c_k$. This, however, is not surprising as the defect atom will have a characteristic dynamical frequency that differs from the symmetric dipole-dipole coupling induced frequency $\propto J$, which the final value theorem we have invoked is resolving.

3. Generic dipole-dipole coupling

If we consider the Hamiltonian associated with N atoms that have generic dipole-dipole coupling, it is of the form

$$\tilde{H}_I = i\sum_{i,\lambda} g_\lambda (a_\lambda \sigma_i^+ e^{i(\omega_0-\omega_\lambda)t} - a_\lambda^\dagger \sigma_i^- e^{-i(\omega_0-\omega_\lambda)t}) + \sum_{i,j\neq i} J_{ij}\sigma_i^+\sigma_j^-, \quad \text{(A24)}$$

where we require that $J_{ij} = J_{ji}$ and $J_{ii} = 0$ to ensure unitary evolution. If we solve the Schrödinger dynamical equations for the state amplitudes we have

$$s\tilde{c}_i = c_i(0) - \sum_j iJ_{ij}\tilde{c}_j - \tilde{G}\sum_j \tilde{c}_j, \quad \text{(A25)}$$

and we may rewrite this as a matrix equation in the form

$$s\vec{\tilde{c}} = \vec{c}(0) - M\vec{\tilde{c}}, \quad \text{(A26)}$$

where $\vec{\tilde{c}}$ is the N dimensional vector with $\vec{\tilde{c}}_i = \tilde{c}_i$, $\vec{c}_i(0) = c_i(0)$ and the coupling matrix

$$M_{ij} = iJ_{ij} + \tilde{G}. \quad \text{(A27)}$$

Thus, in order to solve the more generic case, we need only solve the set of linear equations generated, a scheme that is amenable to computational approaches.

4. Nearest-neighbor coupling

We start with the interaction Hamiltonian for the nearest-neighbor coupling, wherein the atoms only couple to those to either side of them; such an interaction Hamiltonian is of the form

$$\tilde{H}_I = i\sum_{i,\lambda} g_\lambda (a_\lambda \sigma_i^+ e^{i(\omega_0-\omega_\lambda)t} - a_\lambda^\dagger \sigma_i^- e^{-i(\omega_0-\omega_\lambda)t}) + \sum_{j=1}^{N-1} J(\sigma_j^+\sigma_{j+1}^- + \sigma_j^-\sigma_{j+1}^+). \quad \text{(A28)}$$

By performing a similar process as for the symmetric case we find that the coupled differential equations of motion are

$$\dot{c}_\lambda = -g_\lambda e^{-i(\omega_0-\omega_\lambda)t}c_+, \quad \text{(A29)}$$

$$\dot{c}_i = -iJ[(1-\delta_{N,i})c_{i+1} + (1-\delta_{1,i})c_{i-1}] - \int_0^t dt_1 c_+(t_1)G(t-t_1). \quad \text{(A30)}$$

We then integrate up the state amplitudes associated with environment excitations to determine the total polarization parameter

$$\dot{c}_+ = -N\int_0^t dt_1 c_+(t_1)G(t-t_1) - iJ(2c_+ - c_0 - c_N). \quad \text{(A31)}$$

Substituting c_i into itself to second order in the dipole-dipole coupling J yields

$$\tilde{c}_+ = \frac{s^2\tilde{c}_+(0) + iJs[c_1(0) + c_N(0)] + J^2[c_2(0) + c_{N-1}(0)]}{s^3 + (N\tilde{G} + 2iJ)s^2 - 2iJ\tilde{G}s + 2J^2\tilde{G}} \tag{A32}$$

leading to the equation for the atom 1 excited-state amplitude

$$\tilde{c}_1(s) = \frac{s^2c_1(0) - iJsc_2(0) - J^2c_3(0)}{(s^2 + J^2)s} + \frac{\tilde{c}_+(s)\tilde{G}(s)(J^2 + iJs - s^2)}{(s^2 + J^2)s}, \tag{A33}$$

and for atom N

$$\tilde{c}_N(s) = \frac{s^2c_N(0) - iJsc_{N-1}(0) - J^2c_{N-2}(0)}{(s^2 + J^2)s} + \frac{\tilde{c}_+(s)\tilde{G}(s)(J^2 + iJs - s^2)}{(s^2 + J^2)s}. \tag{A34}$$

5. Nearest-neighbor differential ends

We start with the interaction Hamiltonian for the nearest-neighbor coupling, wherein the atoms only couple to those to either side of them; however, the first and last atom in the chain have a transition energy $\omega_0 + 2\delta$ and ω_0, respectively, with the intermediate atoms having transition energy $\omega_0 + \delta$. The interaction Hamiltonian is of the form

$$\begin{aligned}\tilde{H}_I =& J\left(\sigma_1^+\sigma_2^- e^{i\delta t} + \sigma_{N-1}^+\sigma_N^- e^{i\delta t} + \sum_{n=2}^{N-2}\sigma_n^+\sigma_{n+1}^-\right) \\ &+ i\sum_\lambda g_\lambda\left(\sigma_1^+ a_\lambda e^{i(\omega+2\delta-\omega_\lambda)t} + \sigma_N^+ a_\lambda e^{i(\omega-\omega_\lambda)t}\right. \\ &\left.+ \sum_{n=2}^{N-2}\sigma_n^+ a_\lambda e^{i(\omega+\delta-\omega_\lambda)t}\right) + \text{H.c.},\end{aligned} \tag{A35}$$

where H.c. represents the Hermitian conjugate. The associated coupled differential equations of motion are given by

$$\begin{aligned}\dot{c}_1 &= -ic_2J\,e^{i\delta t} - \sum_\lambda c_\lambda g_\lambda e^{i(\omega+2\delta-\omega_\lambda)t}, \\ \dot{c}_i &= -iJ(c_{i-1} + c_{i+1}) - \sum_\lambda c_\lambda g_\lambda e^{i(\omega+\delta-\omega_\lambda)t}, \\ \dot{c}_N &= -ic_{N-1}J\,e^{-i\delta t} - \sum_\lambda c_\lambda g_\lambda e^{i(\omega-\omega_\lambda)t}, \\ \dot{c}_\lambda &= -g_\lambda(c_1 e^{-i(\omega+2\delta-\omega_\lambda)t}) + \sum_n c_n e^{-i(\omega+\delta-\omega_\lambda)t} \\ &\quad + c_N e^{-i(\omega-\omega_\lambda)t}, \\ c_\lambda &= -g_\lambda\int_0^t dt_1 e^{-i(\omega-\omega_\lambda)t_1}\left(c_1(t_1)e^{-2i\delta t}\right. \\ &\quad \left.+ \sum_{n=2}^{N-2} c_n(t_1)e^{-i\delta t} + c_N(t_1)\right).\end{aligned} \tag{A36}$$

We define $c_m(t) = \sum_{n=2}^{N-2} c_n$ and moving forward drop order J^2 and higher terms. We also introduce the notation

$$G_j(t) = G(t)e^{i(j-1)\delta t} \tag{A37}$$

and note that $\tilde{G}_j(s + i\delta) = \tilde{G}_{j-1}(s)$. We may now consider the Laplace transform solutions

$$\begin{aligned}\dot{c}_1 &= -iJc_2e^{i\delta t} - \int_0^t dt_1 G_3(t - t_1)\left(c_1(t_1)\right. \\ &\quad \left.+ \sum_{n=2}^{N-2} c_i(t_1)e^{i\delta t_1} + c_N(t_1)e^{2\delta it}\right), \\ s\tilde{c}_1(s) - c_1(0) &= -iJ\tilde{c}_2(s - i\delta) - \tilde{G}_3(s)[\tilde{c}_1(s) \\ &\quad + \tilde{c}_m(s - i\delta) + \tilde{c}_N(s - 2i\delta)], \\ s\tilde{c}_i(s) &= -iJ[\tilde{c}_{i-1}(s) + \tilde{c}_{i+1}(s)] - \tilde{G}_2(s)[\tilde{c}_1(s + i\delta) \\ &\quad + \tilde{c}_m(s) + \tilde{c}_N(s - i\delta)],\end{aligned} \tag{A38}$$

and for convenience we introduce a set of equations to simplify the derivation

$$\begin{aligned}p(s) &= \tilde{G}_2(s)(N - 2) + s + 2iJ\left(1 + \frac{\tilde{G}_2(s)}{s}\right), \\ q(s) &= iJ\left(2\frac{\tilde{G}_2(s)}{s} + 1\right) + (N - 2)\tilde{G}_2(s), \\ \tilde{c}_m(s) &= -\frac{p(s)}{q(s)}[\tilde{c}_1(s + i\delta) + \tilde{c}_N(s - i\delta)], \\ M(s) &= \tilde{G}_1(s)\left(\frac{iJ}{s + i\delta} - 1\right)\left(1 - \frac{p(s + i\delta)}{q(s + i\delta)}\right), \\ \tilde{c}_N(s) &= \frac{M(s)c_1(0)}{s^2 + 2i\delta s - 2(s + i\delta)M(s)} \\ &= \frac{\tilde{G}_1(s)(iJ - s - i\delta)(s + i\delta + iJ)}{(s + i\delta)[q(s + i\delta) + 2\tilde{G}_1(s)]}.\end{aligned} \tag{A39}$$

If we assume a small value for δ such that the rotating wave approximation is valid we have (i.e., dropping δ^2 terms)

$$\tilde{c}_N(s) = \frac{-\tilde{G}_1(s)}{(s + i\delta)^2 + N\tilde{G}_1(s)(s + i\delta) + 2iJ[\tilde{G}_1(s) + (s + i\delta)]}. \tag{A40}$$

This is just a phase shifted version of the same transition energy case we studied previously.

APPENDIX B: INDEPENDENT RESERVOIRS

1. Fully symmetric coupling

We now consider the interaction Hamiltonian for independent reservoirs which requires us to index over the various atoms' reservoir operators. The interaction Hamiltonian then becomes

$$\begin{aligned}\tilde{H}_I =& i\sum_{i\lambda} g_\lambda(a_{i\lambda}\sigma_i^+ e^{i(\omega_0-\omega_\lambda)t} - a_{i\lambda}^\dagger\sigma_i^- e^{-i(\omega_0-\omega_\lambda)t}) \\ &+ \sum_{j\neq i} J\sigma_i^+\sigma_j^-,\end{aligned} \tag{B1}$$

where we have assumed each reservoir to have the same spectrum of modes such that they all couple with strength g_λ and $a_{i\lambda}$ ($a_{i\lambda}^\dagger$) are the annhilation (creation) operators for the λ mode of the ith atom's reservoir. Now we need to consider the wave function taking a different form as we must index the reservoir to which excitations can go; as such we have our total wave function

$$\phi(t) = c_0\psi_0 + \sum_i^N c_i(t)\psi_i + \sum_{i\lambda} c_{i\lambda}(t)\psi_{i\lambda}, \tag{B2}$$

where $\psi_{i\lambda}$ denotes the excitation being in the λ mode of the ith atom's reservoir. The coupled differential equations of motion are then

$$\begin{aligned}
\dot{c}_i &= -iJ(c_+ - c_i) + \sum_\lambda c_{i\lambda} g_\lambda e^{i(\omega_0-\omega_\lambda)t},\\
\dot{c}_+ &= -iJ(N-1)c_+ + \sum_{i\lambda} c_{i\lambda} g_\lambda e^{i(\omega_0-\omega_\lambda)t},\\
\dot{c}_{i\lambda} &= -g_\lambda e^{-i(\omega_0-\omega_\lambda)t} c_i.
\end{aligned} \tag{B3}$$

Formally integrating up $c_{i\lambda}$ with $c_{i\lambda}(0) = 0$ and substituting back in

$$\begin{aligned}
\dot{c}_i &= -iJ(c_+ - c_i) - \int_0^t G(t-t_1)c_i(t_1)dt_1,\\
\dot{c}_+ &= -iJ(N-1)c_+ - \int_0^t G(t-t_1)c_+(t_1)dt_1.
\end{aligned} \tag{B4}$$

Then from this we can determine the Laplace transform solutions,

$$\begin{aligned}
s\tilde{c}_i(s) - c_i(0) &= -iJ[\tilde{c}_+(s) - \tilde{c}_i(s)] - \tilde{c}_i(s)\tilde{G}(s),\\
s\tilde{c}_+(s) - c_+(0) &= -iJ(N-1)\tilde{c}_+(s) - \tilde{c}_+(s)\tilde{G}(s),
\end{aligned} \tag{B5}$$

which gives

$$\tilde{c}_+(s) = \frac{c_+(0)}{s + iJ(N-1) + \tilde{G}(s)}. \tag{B6}$$

Solving then for $\tilde{c}_i(s)$ yields

$$\begin{aligned}
\tilde{c}_i(s) = &\frac{c_i(0)}{s - iJ + \tilde{G}(s)}\\
&- \frac{iJc_+(0)}{[s + iJ(N-1) + \tilde{G}(s)][s - iJ + \tilde{G}(s)]}.
\end{aligned} \tag{B7}$$

APPENDIX C: PHOTONIC CRYSTAL MODEL

1. Single reservoir

For the memory kernel of the reservoir we have [13]

$$\tilde{G}(s) = \beta^{3/2} e^{-i\pi/4}(s - i\Delta)^{-\frac{1}{2}}, \tag{C1}$$

with the dephasing Δ defined by $\Delta = \omega_0 - \omega_I$, where ω_I is the band edge frequency associated with the photonic band gap and β is the coupling strength of the system-reservoir interaction which provides a canonical timescale for the dynamics. Substituting the photonic crystal memory kernel into Eq. (12) yields for the excited-state populations

$$\begin{aligned}
\tilde{c}_i(s) = &\frac{c_i(0)}{s - iJ}\\
&- \frac{c_+(0)[\beta^{3/2}e^{-i\pi/4}(s - i\Delta)^{-\frac{1}{2}} + iJ]}{(s - iJ)[s + iJ(N-1) + N\beta^{3/2}e^{-i\pi/4}(s - i\Delta)^{-\frac{1}{2}}]}.
\end{aligned} \tag{C2}$$

Then by means of the inverse Laplace transform we determine that the full time dynamics are given by

$$\begin{aligned}
c_i(\tau) = &c_i(0)e^{iJ'\tau} - c_+(0)e^{i\Delta'\tau}\sum_{i=1}^5 a_i x_i e^{x_i^2\tau}\\
&\times\left[1 + r_i - r_i\mathrm{Erfc}\left(\sqrt{x_i^2\tau}\right)\right],
\end{aligned} \tag{C3}$$

where $x_{1,2} = \pm e^{i\pi/4}\sqrt{J' - \Delta'}$ with $J' = J/\beta$, $\Delta' = \Delta'/\beta$, and $\tau = t\beta$ being rescaled by the canonical timescale $1/\beta$ and dimensionless. Erfc is the complementary error function with $\mathrm{Erfc}(z) = 1 - \frac{2}{\sqrt{\pi}}\int_0^z e^{-t^2}dt$. We have the coefficients

$$\begin{aligned}
x_3 &= (A_+ + A_-)e^{i\pi/4},\\
x_4 &= (A_+e^{-i\pi/6} - A_-e^{i\pi/6})e^{-i\pi/4},\\
x_5 &= (A_+e^{i\pi/6} - A_-e^{-i\pi/6})e^{3i\pi/4},\\
A_\pm &= N^{1/3}\left[\frac{1}{2} \pm \frac{1}{2}\left(1 + \frac{4\tilde{\kappa}^3}{27N^2}\right)^{\frac{1}{2}}\right]^{\frac{1}{3}},\\
\tilde{\kappa} &= [\Delta' + J'(N-1)],\\
a_i &= (e^{-i\pi/4} + iJ'x_i)\prod_{j\neq i}^N \frac{1}{x_i - x_j},\\
r_i &= \mathrm{csgn}(x_i),
\end{aligned} \tag{C4}$$

with $\mathrm{csgn}(x_i)$ denoting the complex sign function defined as

$$\mathrm{csgn}(x) = \frac{x}{\sqrt{x^2}}. \tag{C5}$$

2. Nearest-neighbor coupling

Substituting the 1D photonic crystal memory kernel from Eq. (35) into Eq. (26) and performing the inverse Laplace transform yields

$$c_N(\tau) = -e^{i\Delta\tau}\sum_{i=1}^N a_i x_i e^{x_i^2\tau}\left[1 + r_i - r_i\mathrm{Erfc}\left(\sqrt{x_i^2\tau}\right)\right], \tag{C6}$$

where x_i are the five complex roots of the equation

$$\begin{aligned}
&x^5 + x^3(2i\Delta + 2iJ) + x^2N\,e^{-i\pi/4} - x(\Delta^2 - 2J\Delta)\\
&\quad + 2iJ\,e^{-i\pi/4} + i\Delta N\,e^{-i\pi/4}\\
&\quad = 0,
\end{aligned} \tag{C7}$$

$r_i = \mathrm{csgn}(x_i)$, and

$$a_i = e^{-i\pi/4}\prod_{j\neq i}^N \frac{1}{x_i - x_j}. \tag{C8}$$

[1] Y. Wang, Y. Li, Z.-q. Yin, and B. Zeng, npj Quantum Inf. **4**, 46 (2018).

[2] R. Van Meter and K. M. Itoh, Phys. Rev. A **71**, 052320 (2005).

[3] I. L. Markov and M. Saeedi, Phys. Rev. A **87**, 012310 (2013).

[4] M. Saeedi and M. Pedram, Phys. Rev. A **87**, 062318 (2013).

[5] P. Shor, in *Proceedings 35th Annual Symposium on Foundations of Computer Science* (IEEE, New York, 1994), pp. 124–134.

[6] D. Dong and I. Petersen, IET Control Theory Appl. **4**, 2651 (2010).

[7] J. R. Petta, A. C. Johnson, J. M. Taylor, E. A. Laird, A. Yacoby, M. D. Lukin, C. M. Marcus, M. P. Hanson, and A. C. Gossard, Science **309**, 2180 (2005).

[8] T. Yamamoto, Y. A. Pashkin, O. Astafiev, Y. Nakamura, and J. S. Tsai, Nature (London) **425**, 941 (2003).

[9] R. McDermott, R. W. Simmonds, M. Steffen, K. B. Cooper, K. Cicak, K. D. Osborn, S. Oh, D. P. Pappas, and J. M. Martinis, Science **307**, 1299 (2005).

[10] H. P. Breuer and F. Petruccione, *The Theory of Open Quantum Systems* (Oxford University Press, Oxford, 2002).

[11] G. M. Moy, J. J. Hope, and C. M. Savage, Phys. Rev. A **59**, 667 (1999).

[12] A. Burgess and M. Florescu, Opt. Mat. Express **11**, 2037 (2021).

[13] M. Florescu and S. John, Phys. Rev. A **64**, 033801 (2001).

[14] S. John and M. Florescu, J. Opt. A: Pure Appl. Opt. **3**, S103 (2001).

[15] S. John and T. Quang, Phys. Rev. A **50**, 1764 (1994).

[16] G. A. L. White, C. D. Hill, F. A. Pollock, L. C. L. Hollenberg, and K. Modi, Nat. Commun. **11**, 6301 (2020).

[17] H. J. Kimble, Nature (London) **453**, 1023 (2008).

[18] P. Kómár, E. M. Kessler, M. Bishof, L. Jiang, A. S. Sørensen, J. Ye, and M. D. Lukin, Nat. Phys. **10**, 582 (2014).

[19] N. Mirkin, P. Poggi, and D. Wisniacki, Phys. Rev. A **99**, 062327 (2019).

[20] C. H. Fleming, N. I. Cummings, C. Anastopoulos, and B. L. Hu, J. Phys. A: Math. Theor. **45**, 065301 (2012).

[21] J. Schliemann, A. Khaetskii, and D. Loss, J. Phys.: Condens. Matter **15**, R1809 (2003).

[22] R. Fazio and H. van der Zant, Phys. Rep. **355**, 235 (2001).

[23] D. Porras and J. I. Cirac, Phys. Rev. Lett. **92**, 207901 (2004).

[24] L.-M. Duan, E. Demler, and M. D. Lukin, Phys. Rev. Lett. **91**, 090402 (2003).

[25] J. D. Hood, A. Goban, A. Asenjo-Garcia, M. Lu, S.-P. Yu, D. E. Chang, and H. J. Kimble, Proc. Natl. Acad. Sci. USA **113**, 10507 (2016).

[26] S.-P. Yu, J. A. Muniz, C.-L. Hung, and H. J. Kimble, Proc. Natl. Acad. Sci. USA **116**, 12743 (2019).

[27] A. Javadi, I. Söllner, M. Arcari, S. L. Hansen, L. Midolo, S. Mahmoodian, G. Kiršanskė, T. Pregnolato, E. H. Lee, J. D. Song, S. Stobbe, and P. Lodahl, Nat. Commun. **6**, 8655 (2015).

[28] I. Sinayskiy, E. Ferraro, A. Napoli, A. Messina, and F. Petruccione, J. Phys. A: Math. Theor. **42**, 485301 (2009).

[29] W. Cui, Z. Xi, and Y. Pan, J. Phys. A: Math. Theor. **42**, 155303 (2009).

[30] Q.-J. Tong, J.-H. An, H.-G. Luo, and C. H. Oh, Phys. Rev. A **81**, 052330 (2010).

[31] C. Chen, C.-J. Yang, and J.-H. An, Phys. Rev. A **93**, 062122 (2016).

[32] H.-P. Breuer, B. Kappler, and F. Petruccione, Phys. Rev. A **59**, 1633 (1999).

[33] H. Z. Shen, X. Q. Shao, G. C. Wang, X. L. Zhao, and X. X. Yi, Phys. Rev. E **93**, 012107 (2016).

[34] K. M. Ho, C. T. Chan, and C. M. Soukoulis, Phys. Rev. Lett. **65**, 3152 (1990).

[35] E. Yablonovitch, T. J. Gmitter, and K. M. Leung, Phys. Rev. Lett. **67**, 2295 (1991).

[36] S. John and T. Quang, Phys. Rev. Lett. **74**, 3419 (1995).

[37] M. Gross and S. Haroche, Phys. Rep. **93**, 301 (1982).

[38] R. H. Dicke, Phys. Rev. **93**, 99 (1954).

[39] P. Pfeifer, Phys. Rev. A **26**, 701 (1982).

[40] L. Allen and J. H. Eberly, *Optical Resonance and Two-level Atoms*, Dover Books on Physics and Chemistry (Dover, 1987).

[41] B. M. Garraway, Phys. Rev. A **55**, 2290 (1997).

[42] J. Plemelj, Monatsh. Math. Phys. **19**, 205 (1908).

[43] H. Kim, I. Kim, K. Kyhm, R. A. Taylor, J. S. Kim, J. D. Song, K. C. Je, and L. S. Dang, Nano Lett. **16**, 7755 (2016).

[44] L. F. Santos, J. Phys. A **37**, 4723 (2004).

[45] A. Gubin and L. F. Santos, Am. J. Phys. **80**, 246 (2012).

[46] L. A. Pachón, J. D. Botero, and P. Brumer, J. Phys. B: At., Mol., Opt. Phys. **50**, 184003 (2017).

[47] S. John and J. Wang, Phys. Rev. Lett. **64**, 2418 (1990).

[48] H. S. Dutta, A. K. Goyal, V. Srivastava, and S. Pal, Photon. Nanostruct. - Fund Appl. **20**, 41 (2016).

[49] A. Goban, C.-L. Hung, J. D. Hood, S.-P. Yu, J. A. Muniz, O. Painter, and H. J. Kimble, Phys. Rev. Lett. **115**, 063601 (2015).

[50] H.-P. Breuer, E.-M. Laine, and J. Piilo, Phys. Rev. Lett. **103**, 210401 (2009).

[51] A. Burgess and M. Florescu, Dataset for Non-Markovian dynamics of a single excitation within many-body dissipative systems, figshare (2022), https://doi.org/10.6084/m9.figshare.19891759.